SYNTHESIS, CHARACTERIZATION AND CATALYTIC ACTIVITY OF UiO-66-NH_2 IN THE LEVULINIC ACID ESTERIFICATION

Bravo Fuchineco Daiana A.[a]* Heredia Angélica C.[a], Bálsamo Nancy F.[a], Mendoza Sandra M.[b], Arguello Dalma S.[a], Gerbaldo María Verónica.[a], Rodríguez Castellón Enrique[c], Crivello Mónica E.[a]

[a] *Centro de Investigación y Tecnología Química (CITeQ) / Consejo Nacional de Investigaciones Científicas y Técnicas (CONICET) / Universidad Tecnológica Nacional - Facultad Regional Córdoba (UTN-FRC),Córdoba, Argentina.*

[b] *Universidad Tecnológica Nacional / Consejo Nacional de Investigaciones Científicas y Técnicas (CONICET) / Facultad Regional Reconquista, Reconquista 3560, Argentina.*

[c] *Departamento de Química Inorgánica, Cristalografía y Mineralogía / Universidad de Málaga (UMA), Málaga, España.*

**E-mail: dbravo@frc.utn.edu.ar*

Resumen

Como resultado de la explotación masiva del petróleo y su agotamiento, el estudio de materias primas alternativas para reacciones orgánicas provenientes de biomasa, es una tendencia de investigación en la actualidad. En este contexto, el presente trabajo plantea la reacción catalítica de esterificación del ácido levulínico, molécula plataforma, con etanol. Para ello se han sintetizado compuestos del tipo MOF UiO-66-NH_2, con circonio como precursor metálico y ácido aminotereftálico como agente ligante orgánico, empleando una ruta alternativa de síntesis, con condiciones más favorables desde el punto de vista económico y ambiental. Se propone el uso de disolventes alternativos para la síntesis, reemplazando la dimetilformamida por un 25, 50 y 75% de acetona. Las propiedades fisicoquímicas de los materiales se evaluaron por DRX, SEM, FTIR, XPS, MP-AES, medición de acidez y adsorción de N_2 para comprender su estructura cristalina, morfología y estructura porosa. El progreso de la reacción se siguió por cromatografía gaseosa y espectroscopia de masas. El $MOF_{50\%}$ mostró una selectividad a producto deseado de 51.34% y un valor de TON (moles de producto/mol de Zr en el catalizador) de 14.2 en condiciones óptimas, minimizado la masa de catalizador y promoviendo un proceso más económico y eco-compatible.

Palabras clave: Red metal-orgánica (MOF), UiO-66-NH_2, solvotermal, ácido levulínico, esterificación.

Abstract

The massive use of petroleum and its depletion promoted current research trend to the study of alternative raw materials from biomass for organic reactions. In this context, the present work studied the catalytic reaction of esterification of levulinic acid, platform molecule, with ethanol. The MOF type compounds UiO-66-NH_2 have been synthesized. Zirconium was incorporated as metal precursor together with 2-aminoterephthalate acid as an organic binding agent. An alternative route of synthesis was proposed using more favorable conditions since an economic and environmental point of view, replacing dimethylformamide by 25, 50 and 75% acetone as substitute solvent. The physicochemical properties of the materials were evaluated by XRD, SEM, FTIR, XPS, MP-AES and N_2 adsorption to understand its crystalline structure, morphology and porous structure. The progress of the reaction was followed by gas chromatography and mass spectroscopy. The $MOF_{50\%}$ showed a 51.34% of selectivity to the desired products and 14.2 of the turn over number (TON) (moles of product/moles of Zr in the catalyst) by optimal conditions, minimizing catalyst mass and promoting a more economical and eco-friendly process.

Keywords: Metal-organic framework (MOF), UiO-66-NH_2, solvothermal, levulinic acid, esterification.

Quiero expresar el deseo de que este trabajo sea evaluado por el comité para el volumen especial dedicado al CICAT 2020 en alguna de las revistas internacionales: Catalysis Today o Topics in Catalysis.

1. Introduction

The growing demand for chemicals and energy, along with the decline in oil sources, has led to great efforts in the development of renewable replacements for fossil raw materials. The transformation of lignocellulosic biomass into the production of platform molecules became a key role in the development of products with greater added value, which constitutes a crucial step towards the sustainable development of resources [1]. The levulinic acid derived from biomass is considered a building block due to its highly versatile structure for later transformation into different valuable chemical products [2]. In particular, the levulinate esters have low toxicity, high lubricity, flash point stability and moderate flow properties under low temperature conditions, which make them suitable additives for fuels [3]. Ethyl levulinate is usually synthesized using homogeneous acid catalysts such as H_2SO_4, HCl and H_3PO_4 causing inconvenience in catalyst recycling, products separation and environmental problems. The solid acid catalysts are an interesting alternative to overcome the drawbacks of homogeneous ones; they can be easily separated from reaction mixtures and reused for repeated tests [4].

The Metal-organic frameworks are organic-inorganic hybrid crystalline porous materials that consist of a regular array of positively charged metal ions surrounded by organic 'linker' molecules. The metal ions form nodes that bind the arms of the linkers together to form a repeating, cage-like structure. Due to this hollow structure, MOFs have an exceptional large internal surface area [5, 6]. The hybrid composition of inorganic / organic nature gives them characteristics and properties of both inorganic materials such as zeolites, and organic polymeric materials, presenting an ordered crystalline structure together with a high porosity. An exceptional challenge in MOF synthesis is to modify chemical composition, functionality, and molecular dimensions systematically without altering the original topology [7, 8].

The UiO-66-NH_2 material developed by Kandiah et al. was designed by metal clusters composed of six zirconium atoms $Zr_6O_4(OH)_4$, joined together with groups of μ_3-O and μ_3-OH, from the organic ligand 2-aminoterephthalate [9]. This MOF has a three-dimensional porous structure consisting of 9 Å octahedral porous cavities, connected with each other through windows of 6 Å diameters. The high degree of coordination of the metal cluster gives the MOF a high chemical stability [10, 11].

The aim of this work is to evaluate the activity of organic-metal framework (MOFs) in reactions of fine chemistry, such as the esterification of levulinic acid with ethanol. For this purpose, the MOF Zr-UiO-66-NH_2 was synthesized by the solvothermal method, varying the concentration of the solvent. Improvements were applied to the synthesis method to obtain a material with high catalytic performance under more eco-friendly conditions.

2. Experimental

2.1 Reagents

All solutions were prepared with ultrapure water (18 MΩ cm) from a Millipore Milli Q system (DI water). Analytical grade reagents: $ZrCl_4$ (Merck, ≥98%), aminotereftalic acid (NH_2-BDC, Aldrich, 98%), N,N-dimetilformamide (DMF, Biopack, ≥99.8%), Acetone (Sintorgan, 99.5%), Ethanol (Biopack), Levulinic Ácid (Aldrich, 98%) were employed as received.

2.2 Synthesis of MOFs

MOFs were obtained by solvothermal method [12, 13]. The DMF was replaced from 25 to 100 % V/V by acetone. The samples were named as MOF $_{X\%}$ where “X” is the DMF content.

The synthesis consisted of dissolving 1.027 g of $ZrCl_4$ in 50 mL of the solvent (DMF or DMF/ acetone); the solution was magnetically stirred for 5 minutes. Then, 0.789 g of aminoterephthalic acid (NH_2-BDC) were incorporated. The mixture was kept under magnetic stirring for 30 minutes. The gel was transferred into Teflon-lined stainless-steel autoclave and kept in an oven at 120 °C for 24 h. The material obtained was immersed in DMF and then washed with acetone, in order to exchange the DMF for a solvent with a lower boiling point, which can be easily removed. The solid was separated by filtration, obtaining a yellow powdery solid. Finally, the material was dried at 90 °C for 24 h.

2.3 Characterization

The XRD powder patterns were collected on an X’pert diffractometer (PANanalytical, Netherlands) using monochromatized Cu Kα radiation (λ= 1.54 Å) at a scan speed of ¼ ° min^{-1} in 2θ. Infrared analyses were carried out on a

spectrophotometer Smartomi-Transmission Nicolet iS10 Thermo Scientific in a range of 4000-400 cm^{-1}. The micrographs of the mixed oxides were obtained by SEM instrument model JSM-6380 LV (JEOL, Japan) equipped with a Supra 40 (Carl Zeiss, Germany), the samples were metallized with chromium.

The SSA analysis was carried out in an ASAP 2020 instrument (Micromeritics, USA) and was calculated by the Brunauer–Emmett−Teller (BET) method. Prior to the determination of the adsorption isotherms, the precursors were treated at 200 °C during 60 min under 1.0×10^{-3} mbar vacuum.

The X-ray photoelectron spectroscopy (XPS) analysis was carried out using a Thermofisher Scientific K- alpha analysis instrument equipped with a dual X-ray source Mg/Al. High-resolution spectra were recorded in the constant pass energy mode at 30 eV with Mg anode operated at 100 W. The pressure in the analysis chamber was maintained at values below 10^{-9} mbar.

The elemental analysis was carried out by microwave plasma-atomic emission spectroscopy (MP-AES) in an Agilent 4200 instrument (Agilent, USA). Prior to elemental analysis, the samples were dissolved by acid digestion in a microwave oven (SCP Science, Canada).

To assess surface acidity, the CO adsorbed during 2 hours at room temperature was measurement by FTIR analysis at 50 and 100 °C in a Nicolet iS10 instrument.

2.4 Catalytic esterification reaction

The Zr-MOFs were catalytic evaluated in the esterification reaction (1), levulinic acid and ethanol (molar ratio 1:15) were put in contact with a 0.05 g of catalyst in a batch reactor with reflux condenser and in a bath at 78 °C and magnetic stirring [14]. The reaction mixture were analyzed by gas chromatography in a Agilent Technologies 7820A instrument equipped with a HP-20M column and FID detector and by mass spectroscopy in a Perkin Elmer Clarus 560 instrument.

$$C_5H_8O_3 + C_2H_5OH \rightarrow C_7H_{12}O_3 + H_2O \qquad (1)$$

3. Results and discussion

3.1 Physicochemical characterization

Figure 1 shows the X-ray diffraction patterns of the MOFs with different DMF contents (25 to 100%). Two peaks located near 2θ of 7.4° and 8.5° are associated to the diffraction by (111) and (200) planes characteristic of the MOF UiO-66-NH_2. The diffraction patterns show similar behaviors, independently of the substitution of the DMF solvent by acetone [15, 16].

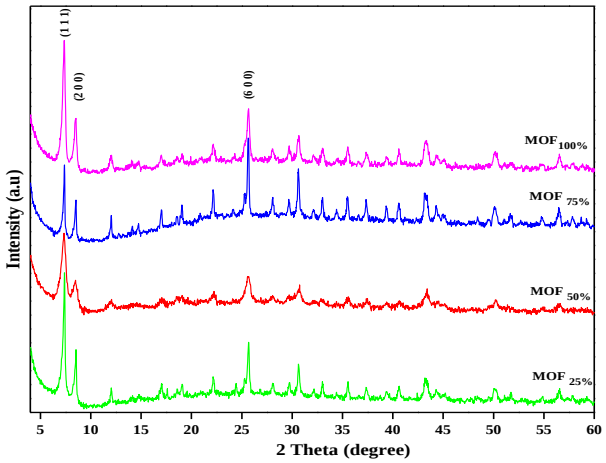

Figure 1. X-ray diffraction patterns for MOFs with different DMF contents.

The MOFs FTIR spectra are shown in Figure 2. The signals at 3447 and 3354 cm^{-1} corresponded with the amine symmetric and asymmetric stretching bands while the signals 1257 and 1385 cm^{-1} were attributed to C-N binding absorption. The COO^- group presented bands at 1571 and 1436 cm^{-1}, assigned to the symmetric and asymmetric stretching vibrations and the C=C benzene ring showed a band at 1494 cm^{-1}. The two lowest frequency at 573 and 475 cm^{-1} were assigned to stretching Zr-O in the MOF clusters. [17].

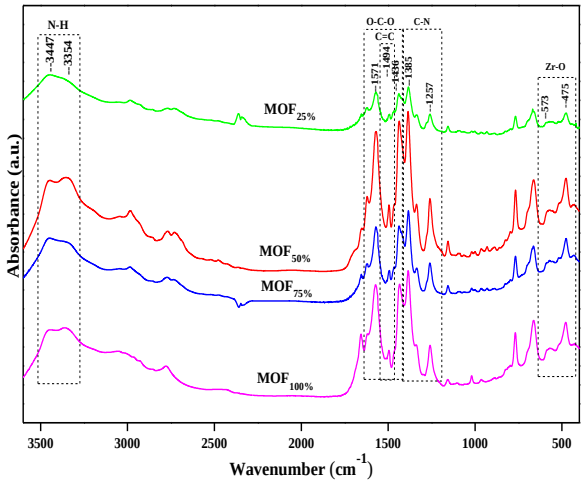

Figure 2. FTIR spectra for MOFs with different DMF contents.

The SEM images of UiO-66-NH_2 showed symmetric pyramid-shaped crystals with a

triangular base, with an average particle size of approximately 200 nm that are similarly at MOF materials (Fig. 3). The $MOF_{100\%}$ crystals are smaller and more dispersed than those obtained by replacing DMF for acetone, in which the small crystals agglomerate constituting a well-defined sphere topology [18].

Elemental mapping verified the presence and dispersion of de Zr, O y C. Figure 4 shows images corresponding to the homogeneous distribution of Zr above the surface in the $MOF_{100\%}$, as well as the presence of Cl atoms that belong to the metal salt and those N atoms contributed by the organic ligand. In the rest of the samples, the dispersion of the elements on the surface was similar.

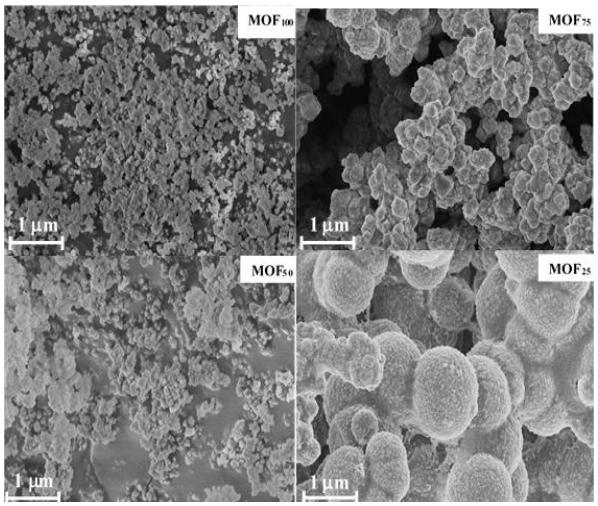

Figure 3. SEM image of the synthetized samples.

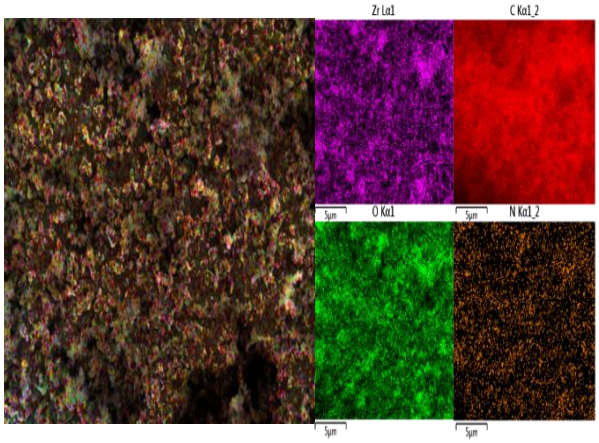

Figure 4. SEM elemental mapping of the $MOF_{100\%}$ sample.

Table 1 shows the content of Zr (% w/w) in the synthesized samples. In most cases the Zr content was approximately 54-66% of the theoretical value (31% w/w). While the $MOF_{25\%}$ sample presented half of the Zr theoretical content.

Table 1. Composition and surface analysis

Catalyst	Zr (%w/w) MP-AES	BET (m^2g^{-1})	Pore size (nm)	Pore volume (cm^3g^{-1})
$MOF_{100\%}$	20.47	399	3.60	0.19
$MOF_{75\%}$	19.72	463	1.13	0.31
$MOF_{50\%}$	21.00	268	2.34	0.23
$MOF_{25\%}$	16.84	255	1.15	0.15

The highest values of surface areas were observed in the $MOF_{75\%}$ and $MOF_{100\%}$ samples (Table 1). Up to $MOF_{75\%}$ a tendency to increase the surface area with DMF content was observed. This effect can also be observed with SEM images where the structures become more compact and closed with the increase of the acetone content. From the adsorption data analysis, it has been observed that these materials are microporous and mesoporous. The physisorption isotherms behavior of the MOFs, according to the IUPAC classification, can be assigned to type Ib, with H4 hysteresis loops that are often found in micro-mesoporous materials. The pore size distribution presented a wide range values between ~1 and ~3 nm and was associated to micro and mesoporosity in the materials (Fig. 5) [19].

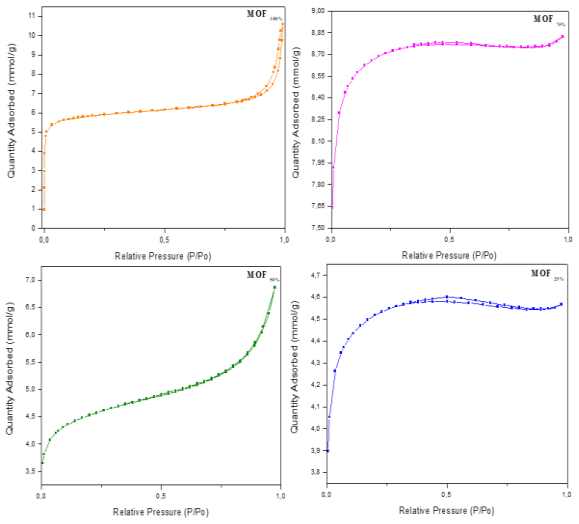

Figure 5. N_2 adsorption−desorption isotherms.

The XPS spectra, presented in Figure 6, confirmed the presence of C, O, and Zr in the samples. The binding energy peaks of Zr $3d_{5/2}$ and $3d_{3/2}$ at around 182.9 and 185.2 eV are attributed to the Zr^{4+} in O-Zr-O environment [20, 21]. Carbon is found in the organic matrix (aminoterephthalic acid), with contributions due to C-C, C=C, C-O and O=C-O bonds. Adventitious carbon is always present. A broad low binding energy contribution at 530 eV in the

O 1s spectrum is assigned to lattice oxygen from Zr oxide and carboxylate oxygen, while the contributions at about 533 and 535 eV are due to C-O bonds and H_2O, respectively.

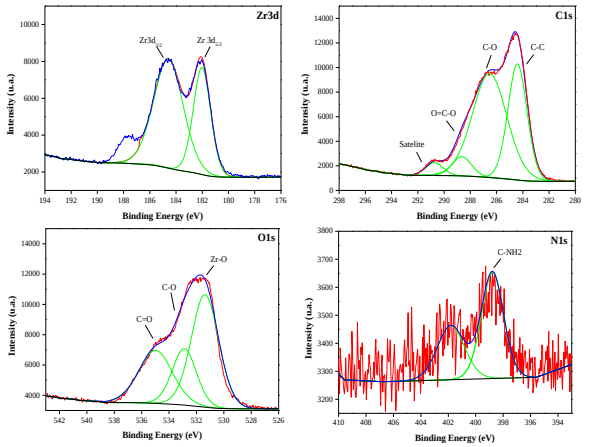

Figure 6. XPS of the Zr 3d, C1s, O1s and N1s regions in the $MOF_{100\%}$.

Finally, the N 1*s* core level spectrum shows two contributions at about 399 and 401.5 eV due to linked amino and protonated amino groups, respectively.

Table 2 shows the relative area percentage corresponding to Lewis and Brønsted acid sites measured by FTIR CO adsorbed at different temperatures (50 and 100 °C). The acid sites measured at low temperature are defined as weak ones while those measured at high temperature are defined as medium ones.

Table 2. FTIR of CO absorbed

Sample	% Area (50°C) Weak sites		% Area (100 °C) Medium sites	
	Lewis	Brønsted	Lewis	Brønsted
MOF 100%	46.97	53.03	50.23	49.77
MOF 75%	55.38	44.62	62.15	37.85
MOF 50%	69.32	30.68	50.29	49.71
MOF 25%	61.17	38.83	55.56	44.44

3.2 Catalytic activity

The esterification products were identified by gas chromatography with FID and mass spectroscopy. The main esterification product was ethyl levulinate (EL) and the byproduct was β-lactone from the dehydration of levulinic acid. The $MOF_{50\%}$ presented the best yield to the EL (Table 3). This behavior can be correlated with the percentage of weak Lewis acid sites associated with highest Zr content, added to the presence of crystalline defects which lead to an increase a pore volume of the material [22]. This structure facilitates the molecules diffusion inside the pores and reaches in internal active sites, improving the catalytic performance. Therefore, some experimental variables were modified, in order to increase the desired product yield.

Table 3. Catalytic activity. T = 78 °C, 0.05 g.

Catalyst	Conversion %	Selectivity EL %	Yield %
$MOF_{100\%}$	12.85	40.75	5.23
$MOF_{75\%}$	21.01	41.97	8.81
$MOF_{50\%}$	20.07	46.66	9.36
$MOF_{25\%}$	18.37	24.65	4.52

The reaction temperature was modified to 85 °C, and 0.1 g (2W), 0.025 g (1/2 W) and 0.0125 g (1/4 W) of catalyst were tested. On the other hand, prior to the reaction, the catalyst was washed with ethanol (EW) to take out possible solvent presence in the pores. Finally, the reaction was carried out with the following combined variables: 85 °C, 1/2 W and EW, called optimal conditions (OC). The TON was defined as moles of LA converted to EL (yield to EL) / (mole of Zr). Table 4 shows that the $MOF_{50\%}$ tested in OC achieved the highest TON value. Highlighting that the catalyst mass was reduced by the half, thus promoting the favorable interaction between the substrate and the catalyst surface.

Table 4. Catalytic activity of $MOF_{50\%}$ T = 85°C

MOF 50%	Conversion %	Selectivity %	Yield %	TON
W	23.95	51.82	12.41	6.9
2W	17.48	44.77	7.82	2.18
½ W	20.87	44.43	9.27	10.3
¼ W	13.27	41.02	5.44	12.08
OC	24.89	51.34	12.77	14.2

4. Conclusions

The synthesis of MOF UiO-66-NH_2 phases were achieved under mild solvothermal conditions, replacing up to 75% v/v of the traditional dimethylformamide by acetone. XRD and SEM analyses showed good crystalline and morphology in the synthesized samples. The Zr^{4+} species coordinated in an O-Zr-O environment was observed by XPS analysis. The pore size between ~1 and ~3 nm was measured and associated to micro and mesoporosity in the materials. The

weak and medium acid sites of Lewis and Brønsted were identified by FTIR of adsorbed CO.

The catalytic activity showed that TON values increased markedly with the decreasing catalyst mass, which would confirm that, a high interaction between substrates and the Lewis acid contributed by the available Zr^{4+} inside the pore and on the catalyst surface, promote the esterification reaction. Therefore the optimal conditions with a high EL yield was obtained, minimizing catalyst mass and promoting a more economical and eco-friendly process.

5. Acknowledgments

Financial support from the Consejo Nacional de Investigaciones Científicas y Tecnológicas (CONICET) and Universidad Tecnológica Nacional – Facultad Regional Córdoba (UTN-FRC). The autor thanks to Mass spectroscopy laboratory INFIQC-CONICET. ERC thanks to projects RTI2018-099668-BC22 of Ministerio de Ciencia, Innovación y Universidades, and UMA18-FEDERJA-126 of Junta de Andalucía and FEDER funds.

6. References

[1] Mikola, M., Ahola, J., & Tanskanen, J., Chemical Engineering Research and Design, 148 (2019) 291–297.

[2] Lin, T.Y., Lin, K.Y. A., Journal of the Taiwan Institute of Chemical Engineers, 96 (2019) 321–328.

[3] Isao Ogino, Yukei Suzuki and Shin R.Mukai, Catalysis Today, 314 (2018) 62-69.

[4] Tianmeng Guo, Mo Qiu, Xinhua Qi, Applied Catalysis A: General, 572 (2019) 168-175.

[5] Llorente P. L, Síntesis y aplicación catalítica de materiales MOF en reacciones de química fina, Universidad Rey Juan Carlos, Móstoles, 2017.

[6] Norbert Stock and Shyam Biswas, American Chemical Society, 112 (2012) 933-969.

[7] Jesse L.C. Rowsell and Omar M. Yaghi. American Chemical Society, 73 (2004) 3-14.

[8] Yujia Sun & Hong-Cai Zhou, Science and Technology of Advanced Materials, 16:5 (2015), 054202.

[9] Kandiah M., Nilsen MH, Usseglio S., Jakobsen S., Olsbye U., Tilset M., Larabi C., Quadrelli EA, Bonino F., Lillerud KP. Chemistry of Materials, 22, 24 (2010) 6632–6640.

[10] Abid, H. R., Shang, J., Ang, H.M., & Wang, S., International Journal of Smart and Nano Materials, 4 (2013), 72–82.

[11] Yan Cao, Hongmei Zhang, Fujiao Song, Tao Huang, Jiayu Ji, Qin Zhong, Wei Chu and Qi Xu, Materials 11 (2018), 589.

[12] Garibay, S. J., & Cohen, S. M., Chemical Communications, 46 (2010) 7700.

[13] L. Lozano, C. Iglesias, B. Faroldi, M. Ulla y J. Zamaro, Journal of Materials Science, 53 (2018) 1862-1873.

[14] F. G. Cirujano, A. Corma, F. X. Llabrés i Xamena, Chemical Engineering Science 124 (2015) 52-60.

[15] Lin, K.Y. A., Liu, Y.T., & Chen, S.Y., Journal of Colloid and Interface Science 461 (2016) 79–87.

[16] Huang, A., Wan, L., & Caro, J., Materials Research Bulletin 98 (2018) 308–313.

[17] Ubed SF Arrozi, Husni W. Wijaya, Aep Patah, Yessi Permana, Applied Catalysis, 506 (2015) 77-84.

[18] Yitong Han, Min Liu, Min Liu, Keyan Li, Xinwen GuXinwen Guo, CrystEngComm 17 (2015) 6434.

[19] Abid, H. R., Shang, J., Ang, H.-M., & Wang, S., International Journal of Smart and Nano Materials 4 (2013) 72–82.

[20] Bibi R., Shen Q., Wei L., Hao D., Li N., Zhou J., Royal Society of Chemistry, 8 (2018) 2048.

[21] Xu W., Dong M., Di L., Zhang X. Nanomaterials, 9 (2019) 1432.

[22] DeStefano M. R., Islamoglu T., Garibay S. J., Hupp J. T. , Farha O. K., Chemistry of Materials 29,3 (2017) 1357-1361.